Design and Implementation of a Quasi-Orthogonal Switching Beam-Former for Triangular Arrays of Three Radiating Elements

Javier García-Gasco Trujillo, Álvaro Noval Sánchez de Toca, Ignacio Montesinos Ortego, José Manuel Fernández González, and Manuel Sierra Pérez

Abstract—**An innovative switching multi-beam network for triangular arrays of three radiating elements is proposed. This novel network provides three orthogonal beams in a desired elevation angle and a fourth one in the broadside steering direction. The network is composed of four-port 3-dB quadrature hybrid power couplers and fixed phase shifters. In this paper, a relation between network components, radiating element distance and beam steering directions is shown. Application of the proposed dissipative network to the triangular cell of three double stacked patches of 1.7 GHz and 60° beamwidth that integrates the intelligent antenna GEODA with an array distance of 0.56λ is exhibited. Measured scattering parameters of the network are compared with both, theoretical and simulated scattering matrices, validating the expected behavior. Besides, by combining two complementary single proposed networks, a matrix that supplies six orthogonal beams in a given elevation angle and a seventh one in the broadside steering direction has been built. Moreover, the whole system, dissipative network with GEODA cell array, has been measured in the anechoic chamber of the Radiation Group at Technical University of Madrid, demonstrating a successful performance.**

Index Terms—**Adaptive arrays, beam steering, multibeam antennas, phased arrays.**

I. Introduction

FROM the beginning of telemetry, tracking and command (TT&C) systems, mechanical scanning antennas have been employed at ground stations. As it is well known, this technique is not only sensitive to gravity and mechanical failure, but also slow, increasing the total cost of the system and making simultaneous satellite communications infeasible. The use of electronically scanned antenna arrays overcomes these limitations, allowing much faster multi-beam scans without physical antenna rotation [1], [2]. These types of systems that use information from the link environment to set the proper beam shape are called intelligent architectures [3], [4].

In order to improve the ground station performance, many studies have been carried out in the field of electronic scanning systems, in which large arrays composed of thousand of radiating elements have been considered [5]. Electronic steering technique is based on the control of the relative amplitude and phase of the signal associated with each antenna that composes the whole array. The relative signal can be adjusted by using digital signal processing algorithms, e.g., MUSIC [6] or ESPRIT [7], or placing beam-forming circuits inside the hardware antenna, e.g., phase shifters [8] or switched networks [9].

Nowadays, software/hardware hybrid architectures are gaining special interest because of their versatility. Generally, these huge array structures are divided into subarrays based on unitary cells of at least three radiating elements to reduce not only post-processing data time but also its cost [10]–[12]. The unitary cell radiation pattern, the combiner/divider cell circuit and the post-processing data algorithm will define the whole system capabilities. This segmentation may reduce the total number of required active circuits, such as amplifiers or phase shifters [13], decreasing total cost and improving post-processing data efficiency. Usually, this type of antenna performs a hardware beam steering that selects the willing communication direction area and a signal data processing algorithm that improves the desired signal to interfering signal/noise rates. Therefore, the study of structures that provide multiple beams in different spatial ranges related to each sub-array cell is needed.

The number of radiating elements composing the unitary cell and its distribution state the basic beam scanning shape. A triangular cell of three radiating elements is the simplest way to obtain a planar scanner. In this paper, a new multibeam network configuration that provides three orthogonal beams in a desired θ_0 elevation angle and an extra one in the broadside steering direction for a triangular array of three radiating elements will be introduced. Section II will present a short introduction to the state of art of classical multi-beam networks [14], [15]. Lossless network analysis, including original lossless network designs [9], will be also commented. Section III will show general dissipative matrices theory as well as applications for array antennas of three radiating elements. In Section IV, the proposed final basic multi-beam network will be simulated, built and measured to the GEODA practical case. Section V will present a combined network that provides six orthogonal beams in a desired θ_0 elevation angle and a double seventh one in the broadside direction by using two complementary proposed basic net-

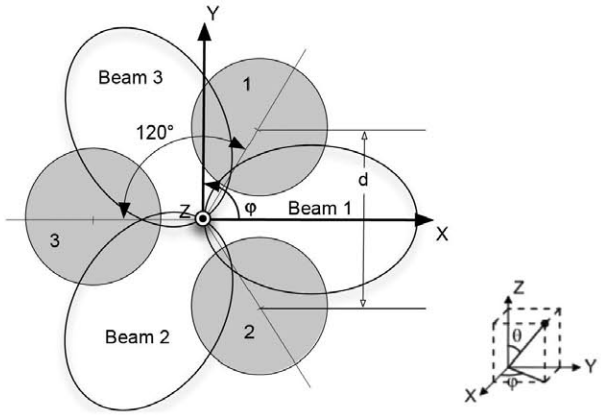

Fig. 1. (Left) Triangular cell of three radiating elements and its orthogonal beams [Azimuth xy-plane]. (Right) Coordinate System.

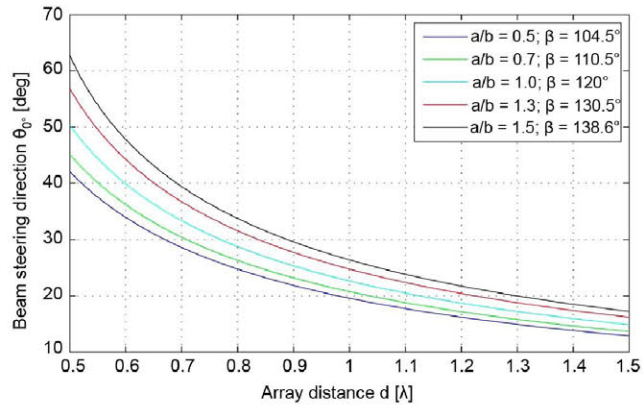

Fig. 2. Array factor steering direction θ_0 respect to array distances for different feeding signal relations.

works. Measurements of the whole system will be also depicted. Finally, Section VI will collect the conclusion drawn during the paper.

II. Orthogonal Multi-Beam Forming Networks for Triangular Arrays

One of the most important tasks in a phased array antenna is to design the beam-forming network (BFN). A BFN essentially combines/divides properly the signal of/to each radiating element compounding the array in order to produce the desired beam. Most common types of BFNs are presented in [13], where Butler matrix [16], Blass network [17], Rotman lens [18] and many more are explained. Many studies have been developed in order to overcome the limitations of these useful networks. As an example, a switching network that generates four beams for three linear radiating elements is presented in [19]. Final network presented in this paper is based on Butler matrix modifications.

The behavior of a BFN is characterized by its scattering matrix. As presented in [9], when a lossless and reciprocal network with adapted and isolated beam and array ports is considered, vectors related to the columns of each transmission and reception matrices are orthonormal to each other. Hence, the number of beam and array ports must be the same; the output power must be equal to the input power; and its scattering matrix vectors must be orthogonal, ensuring isolation between different beams.

Assuming three radiating elements located over vertices of an equilateral triangle in the xy-plane with d side length as in Fig. 1, the relation between the location of the radiating elements and the array signal is shown in (1) and (2)

$$AF(\theta,\phi) = \sum_{i=1}^{3} A_i e^{-j\alpha_1} e^{-jk\hat{r}r_i} \tag{1}$$

$$\begin{aligned} -k\hat{r}r_{patch1} - \alpha_{patch1} &= -k\hat{r}r_{patch2} - \alpha_{patch2} \\ &= -k\hat{r}r_{patch3} - \alpha_{patch3}. \end{aligned} \tag{2}$$

The lossless scattering parameters of a network associated with a triangular cell of three radiating elements that provides three orthogonal beams in a desired θ_0 elevation angle must satisfy the condition of adding contributions of each array element in the desired steering direction. Hence, it is shown that desired beam is obtained when relations between array port signals are

$$S_{patch1,Beam1} = S_{patch2,Beam1} = ae^{-j\alpha} \tag{3}$$

$$S_{patch3,Beam1} = be^{-j(\alpha+\beta)} \tag{4}$$

where

$$\beta = \sqrt{3}\frac{\pi d}{\lambda}\sin(\theta_0). \tag{5}$$

Two additional orthogonal beams are obtained by rotating signal relations between array ports.

Ensuring orthogonal excitation vectors by imposing (2), is obtained,

$$\sin(\theta_0) = \frac{\lambda}{\sqrt{3}\pi d}\arccos\left(\frac{-a}{2b}\right). \tag{6}$$

Beam steering direction θ_0, depends on both, array element distance d and feeding signal relation between elements in amplitude a/b and phase β. Fig. 2 shows the steering elevation direction θ_0 of the array factor for different d, a/b and β. As distance between elements d or relation b/a increase, beam steering direction θ_0 raise closer to broadside ($\theta_0 = 0°$).

Once analysis has been performed, the hard task is to find structures that fulfill the desired behavior. Different lossless schemes of three beam ports by three array ports based on hybrid couplers and fixed phase shifters have been studied, [9]. Intrinsic features of orthogonal lossless networks limit the number of provided beams to the number of radiating elements and impose the relation between those beams. Therefore, this research leads to consider the possibility of using dissipative networks, which are capable of providing a higher number of beams than the number of radiating elements compounding the cell.

III. Dissipative Network for Triangular Arrays

Dissipative networks are those that have intrinsic losses associated with each generated beam. This type of network has no need to accomplish beam orthogonal condition, giving a greater degree of freedom to control beam steering directions. When orthogonal condition is fulfilled in all the beams of a network, the maximum array gain is ensured due to lossless implicitness.

However, when radiating elements are related to radiofrequency circuits in which amplifiers are found, the relevant parameter that shows the quality of the antenna is the G/T factor. As a result, the use of a dissipative network is not restricted whenever there is an amplifier stage.

In this section, a four beam ports by three array ports quasi-orthogonal dissipative network that generates three orthogonal beams in a desired elevation direction θ_0 and an additional beam in the broadside direction is studied. To this end, a four beam ports by four array ports network with a matched array port is analyzed. The scattering matrix associated to the dissipative network under study is shown in (7). Broadside beam is obtained by maintaining same signal relation between elements at array ports (column one). Three orthogonal beams are generated as analyzed in Section II thanks to columns two to four

$$[S_T] = \begin{bmatrix} f & be^{-j\beta} & a & a \\ f & a & be^{-j\beta} & a \\ f & a & a & be^{-j\beta} \\ g_1 e^{j\alpha_1} & g_2 e^{j\alpha_2} & g_3 e^{j\alpha_3} & g_4 e^{j\alpha_4} \end{bmatrix}. \quad (7)$$

The matched array port gives a degree of freedom, as depicted in row four of matrix (7), with which is possible to satisfy the reciprocity lossless condition (2) if the whole 4 × 4 network is considered. This condition does not remove losses associated to the 4 × 3 dissipative network but reduces them to the power absorbed by the matched array port. Applying condition (2) to the scattering matrix (7) is obtained

$$g_1^2 = 1 - 3f^2 \quad (8)$$

$$g_i = 1 - 2a^2 - b^2 \text{ with } i = [2,4] \quad (9)$$

$$f\left(2a + be^{i\beta}\right) = -g_1 g_i(\alpha_1 - \alpha_i) \text{ with } i = [1,2] \quad (10)$$

$$a\left(a + be^{j\beta} + b^{-j\beta} + b^{-j\beta}\right) = -g_i g_j e^{j(\alpha_i - \alpha_j)} \text{ with } i,j = [2,4] \quad (11)$$

Solving system (8)–(11), relation between signal array ports are given by

$$a = \sqrt{\frac{1 - f^2}{2 + r^2}} \quad (12)$$

$$b = ar = r\sqrt{\frac{1 - f^2}{2 + r^2}} \quad (13)$$

where

$$r = \frac{b}{a}. \quad (14)$$

Losses associated with the network are related to the broadside beam as

$$g_1 = 1 - 3f^2 \quad (15)$$

$$g_i = f^2 \text{ with } i = [2,4]. \quad (16)$$

Total mean losses of the 4 × 3 dissipative network is

$$\frac{\sum_{i=1}^{4} d_i^2}{4} = 1 - 3f^2 + 3f^2 = \frac{1}{4}. \quad (17)$$

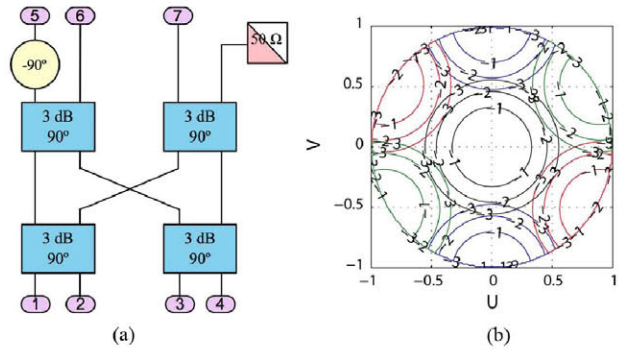

Fig. 3. (a) Scheme of a 4 × 3 modify Butler matrix. (b) GEODA cell array factor when the network is connected. Each color is a different beam.

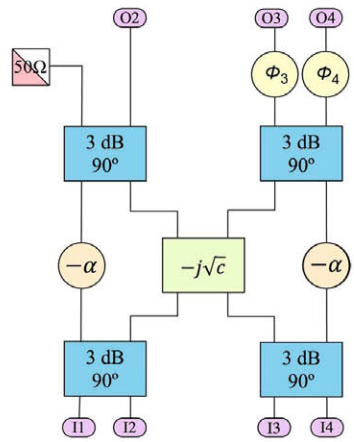

Fig. 4. 4 × 3 proposed dissipative network.

Showing that total mean network losses are independent of its configuration, being a fourth of the total power. The homogeneous losses case is obtained when $f = 1/2$, in which each beam has 1.25 dB losses.

The steering direction of the three orthogonal beams with the desired θ_0 elevation angle depends on signal factors, (a, b), and on the distance between elements of the array, (d), as

$$\sin(\theta_0) = \frac{\lambda}{\sqrt{3}\pi d} \cos^{-1}\left(\frac{a^2 + b^2 - 1}{2ab}\right). \quad (18)$$

Several dissipative networks for triangular arrays have been studied. It is important to bear in mind the fact that the appearance of intrinsic side lobes and diffraction must be considered and avoided, as shown in [9], where the truncated Butler network for three radiating elements shown in Fig. 3(a) was analyzed, presenting two main lobes when it was applied to a triangular cell array. Fig. 3(b) depicts expected array factor if the network is applied to GEODA subarray cell.

Finally, the proposed dissipative network that provides three orthogonal beams in the desired steering direction λ_0 and an additional one in broadside is shown in Fig. 4. The network is composed of four four-port 3 −dB 90° hybrid power couplers, four fixed phase shifters and a $20\log(\sqrt{c})$ dB 90° power coupler. Its behavior is shown in (19) at the bottom of the next page, thanks to its scattering matrix.

To obtain the proper signal network distribution that generates the desired beams, the scattering matrix of the proposed network, (19), must be matched to the desired scattering matrix pattern previously analyzed, (7). After comparison, scattering parameters of the network under study are giving by

$$(\mathrm{mod}[S_T])^2 = \frac{1}{4}\begin{bmatrix} c & 4-3c & c & c \\ 4-3c & c & c & c \\ c & c & c & 4-3c \\ c & c4-3c & c & c \end{bmatrix} \quad (20)$$

$$\arg[S_T] = \begin{bmatrix} -\frac{\pi}{2} & T & -\pi & -\frac{3\pi}{2} \\ T & \frac{\pi}{2} & \frac{-\pi}{2} & T \\ 0 & \frac{\pi}{2} & \frac{-\pi}{2} & T \\ 0 & \frac{\pi}{2} & T & -\pi \end{bmatrix}, T = \tan^{-1}\left(\frac{-2\sqrt{1-c}}{-\sqrt{c}}\right). \quad (21)$$

The behavior of the network is governed by the value of the central coupler c, as shown in (20) and (21). Relations between network components obtained after study are

$$\cos(\alpha) = \sqrt{1-c} \quad \text{with } \sin(\alpha) = \pm\sqrt{c} \quad (22)$$

$$\phi_3 = \phi_4 + \frac{\pi}{0} = -\pi. \quad (23)$$

The sign in $\sin(\alpha) = \pm\sqrt{c}$ determines the desired elevation steering direction $\pm\theta_0$ of the three orthogonal beams. In the above analysis, $\sin(\alpha) = +\sqrt{c}$ has been considered. A complementary beam-former network could be obtained by using in the study $\sin(\alpha) = -\sqrt{c}$, as shown in Section V. Moreover, note that ϕ_3 and ϕ_4 are fixed phase shifters not related to the desired steering direction θ_0 of the three orthogonal beams but to the relative phases between array ports needed to generate the different desired beams.

The relation between the desired steering direction angle θ_0 and the phase shift between elements β was given by (5). The steering direction of orthogonal beams as well as losses associated with each beam depend on the coupler c as

$$\sin(\theta_0) = \tan^{-1}\left(\frac{-2\sqrt{1-c}}{-\sqrt{c}}\right)\frac{1}{\sqrt{3}\pi}\frac{\lambda}{d} \quad (24)$$

$$L_{\theta_0} = -10\log(1-\frac{c}{4}) \quad (25)$$

$$L_{\theta^0} = -10\log(\frac{3}{4}c). \quad (26)$$

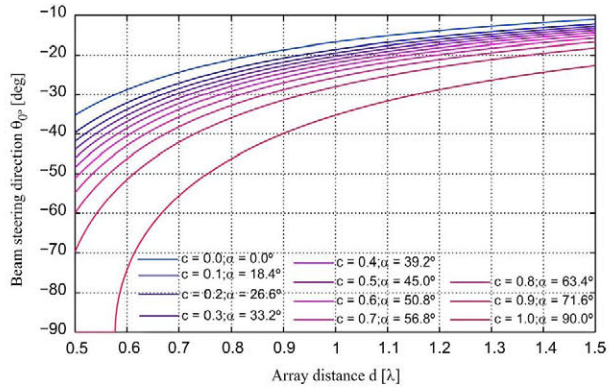

Fig. 5. Beam steering directions θ_0 depending on parameters c, α, and d.

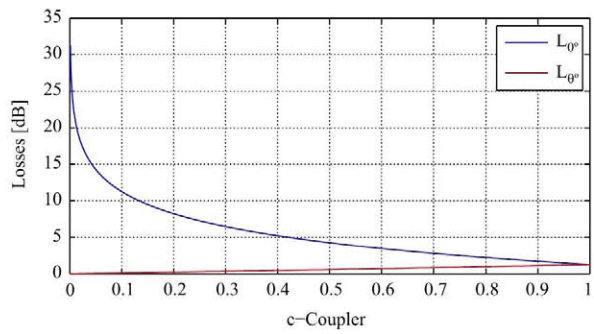

Fig. 6. 4 × 3 Beam losses. (Blue) Broadside beam. (Red) θ_0 steering direction.

Fig. 5 shows beam steering directions θ_0 depending on the parameters c, α and d. Both type of losses, L_{0° and L_{θ_0} associated with broadside and tilted beams respectively, are also depicted in Fig. 6.

Fig. 5 presents the beam steering capabilities of the network, showing that for larger arrays the possible coverage area in the system is reduced. For a beam-switching application, the continuous coverage of the system field-of-view is a critical design requirement, which means that relative amplitudes between every beam compounding the network must be carefully analyzed. The total losses of the system that must be taken into account are: intrinsic losses of the proposed network (Fig. 6) and losses introduced into the tilted beams because of the beam width of the single element composing the antenna array. The important condition in the design is that both losses should be balanced to provide a quasi-homogeneous radiation pattern in the system

$$[S_T] = \frac{1}{2}\begin{bmatrix} A-B & -j(A+B) & -\sqrt{c} & j\sqrt{c} \\ -j(A+B) & -(A-B) & -j\sqrt{c} & -\sqrt{c} \\ -\sqrt{c}e^{-j\phi_3} & -j\sqrt{c}e^{-j\phi_3} & (-(A-B))e^{-j\phi_3} & (-j(A+B))e^{-j\phi_3} \\ j\sqrt{c}e^{-j\phi_4} & -\sqrt{c}e^{-j\phi_4} & (-j(A+B))e^{-j\phi_4} & (A-B)e^{-j\phi_4} \end{bmatrix}$$

$$A = e^{-j\alpha}$$

$$B = \sqrt{1-c} \quad (19)$$

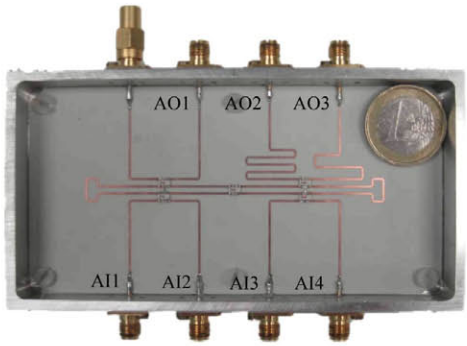

Fig. 7. Microstrip dissipative 4 × 3 proposed network.

field-of-view considered. Losses in software/hardware hybrid architectures are compensated by using amplifiers.

Fig. 6 depicts that the intrinsic network losses for the broadside beam decrease as c increases, showing that for c-coupler smaller than 0.4 the losses for the broadside beam will be higher than 5 dB. Therefore, it is important to notice that to implement a proposed network with such a small c-coupler might be impractical since it would be very difficult to balance such a high intrinsic losses of the network.

IV. Implementation of the Proposed 4 × 3 Network

In this section, a microstrip implementation of the proposed dissipative network is presented. The aim of this section will be to validate that the signal distribution provided by the network is as defined by (20) and (21). The generation of three orthogonal beams with a θ_0 elevation angle and an additional one in the broadside direction when the designed network is applied to a triangular cell of three radiating elements will be verified as well. For this purpose, the simple practical case in which all hybrid power couplers composing the network are four-port 3-dB quadrature couplers is assumed. This case is obtained when main network parameters are

$$c = 0.5 \quad \text{with} \alpha = 45°. \tag{27}$$

To simplify the implementation and minimize the size of the whole network, commercial four-port 3-dB quadrature hybrid power couplers (Mini Circuits QCN-25) are used. Additional fixed microstrip transmission line lengths will generate required phase shifters. Taking (27) into (20) and (21), the scattering matrix associated to this network is

$$\text{mod}[S_T] = \begin{bmatrix} 0.35 & 0.79 & 0.35 & 0.35 \\ 0.79 & 0.35 & 0.35 & 0.35 \\ 0.35 & 0.35 & 0.35 & 0.79 \\ 0.35 & 0.35 & 0.79 & 0.35 \end{bmatrix} \tag{28}$$

$$\arg[S_T] = \begin{bmatrix} -90° & -116.6° & -180° & -270° \\ -116° & 90° & -90° & -180° \\ 0° & 90° & -90° & 63° \\ 0° & 90° & -206.6° & -180° \end{bmatrix}. \tag{29}$$

To check a correct performance, the network with ideal components has been simulated by CST Design Studio 2011. Its scattering matrix shows a perfect behavior. Simulated scattering parameters with real measurements of the 4 × 3 dissipative network components, fixed phase shifters and QCN -25 90°3 dB hybrid couplers, are shown in expressions (30) and (31). These measurements show a good agreement with expectations, with a phase error of ±4° and an amplitude error of ±0.1 dB

TABLE I
Scattering Matrix and Losses of the 4 × 3 NETWORK

	AO1	AO2	AO3	β	Losses
I1	$0.700e^{j0.915\pi}$	$0.305e^{-j0.446\pi}$	$0.302e^{-j0.412\pi}$	118.1°±3°	32%
I2	$0.327e^{j0.032\pi}$	$0.312e^{j0.049\pi}$	$0.300e^{j0.068\pi}$	0°±3°	70%
I3	$0.312e^{-j0.951\pi}$	$0.327e^{-j0.969\pi}$	$0.683e^{j0.417\pi}$	112.1°±2°	33%
I4	$0.312e^{j0.537\pi}$	$0.691e^{-j0.108\pi}$	$0.324e^{j0.572\pi}$	119.1°±3°	32%

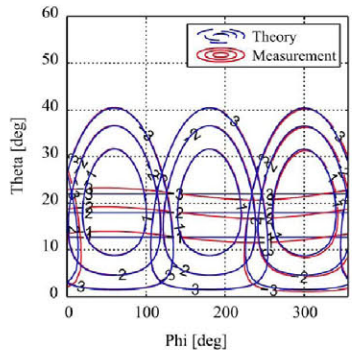

Fig. 8. Radiation pattern simulation of the whole system, cell with proposed network, using theoretical (blue) and measured (red) S-parameters.

$$\text{mod}[S_T] = \begin{bmatrix} 0.30 & 0.72 & 0.31 & 0.30 \\ 0.73 & 0.32 & 0.31 & 0.30 \\ 0.31 & 0.32 & 0.31 & 0.73 \\ 0.30 & 0.31 & 0.72 & 0.31 \end{bmatrix} \tag{30}$$

$$\arg[S_T] = \begin{bmatrix} -87.0° & -114° & -182° & -270° \\ -118° & 94° & -90° & -181° \\ -1° & 87° & -92° & 66° \\ 0° & 86° & -208° & -177° \end{bmatrix}. \tag{31}$$

The network has been implemented in a microstrip RO4350B substrate of 0.254 mm thickness as presented in Fig. 7. Fixed phase shifters and four-port $3-$ dB 90° hybrid power couplers (QCN-25) have been evaluated independently in order to assure a good performance. The use of commercial chip couplers is helpful when total network dimensions must be minimized. The network presents ±0.3 dB module error and ±5° phase error as summarized in Table I. Signal errors introduced are reasonable, as it is depicted in Fig. 8, where a comparative simulation between radiation patterns of the cell GEODA with theoretical and measured S network parameters shows low beam steering deviations. It is worth noting the use in the simulation of the previous measured radiation pattern of the radiating element composing the GEODA cell, which consists of two stacked circular patches with 60° beamwidth [9]. This beamwidth explains not only the mismatch between factor array and radiation pattern elevation steering direction θ_0, shifting from $-41.9°$ to $-23.1°$, but also the increase of side lobes shown in following radiation pattern measurements of the GEODA cell with the implemented network.

Fig. 8 shows an almost continuous coverage by using a patch element with a 60° beamwidth.

Moreover, the whole system, dissipative 4 × 3 network with GEODA cell array, has been measured in the anechoic chamber

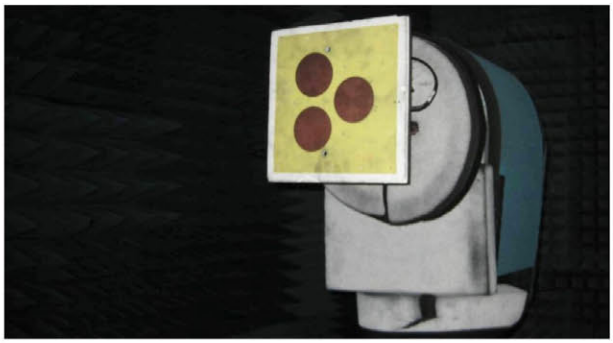

Fig. 9. Whole system, dissipative 4 × 3 network with GEODA cell array, in the anechoic chamber of the Radiation Group at UPM.

of the Radiation Group at Technical University of Madrid as shown in Fig. 9. Measurements confirm the generation of one beam in the broadside steering direction with an error of $\pm 3°$ and three orthogonal beams equidistant in azimuth $120° \pm 5°$ with an elevation of $-23° \pm 2°$, as expected, depicted in Fig. 10. The radiation patterns associated with the three tilted beams present an increased secondary lobe with a peak of -5 dB with respect to the main beam. Comparisons between measured and simulated radiation patterns associated with each beam have shown a good. Main lobe shapes and steering directions fit properly. The three tilted beams present acceptable smooth variations in amplitude, ± 2 dB, and azimuth, $\pm 7.5°$. These deviations might be related to a mismatch between the built and the simulated patch array structure.

V. A 7 × 3 BFN By Using Complementary Networks

To find a beam pattern as homogeneous as possible leads to consider the use of switching beam-formers with higher number of beams. While the number of beams provided by the network is increased, the depointing losses associated with the switching between contiguous beams are reduced. In this section, a new 7 × 3 network is proposed by combining two complementary 4 × 3 networks as described in Fig. 11. The practical implementation is composed of the designed network in the previous section (BFN A) and its complementary network that generates same beams but rotated 180° in azimuth (BFN B).

Design parameters of BFN B are obtained by considering in the analysis the relation (32)

$$\cos(\alpha) = \sqrt{1-c} \quad \text{with} \sin(\alpha) = -\sqrt{c}. \tag{32}$$

Then

$$c = 0.5 \quad \text{with} \alpha = -45° \tag{33}$$

$$\phi_3 = \phi_4 + \frac{\pi}{2} = 0°. \tag{34}$$

Being the expressions governing complementary networks as follow:

$$\beta = -\sqrt{3}\pi \frac{d}{\lambda} \sin(\theta_0) \tag{35}$$

$$\sin(\theta_0) = -\sqrt{\frac{1}{\sqrt{3}\pi}} \frac{\lambda}{d} \left(\tan^{-1} \left(\frac{-2(\sqrt{1-c})}{\sqrt{c}} \right) + \pi \right). \tag{36}$$

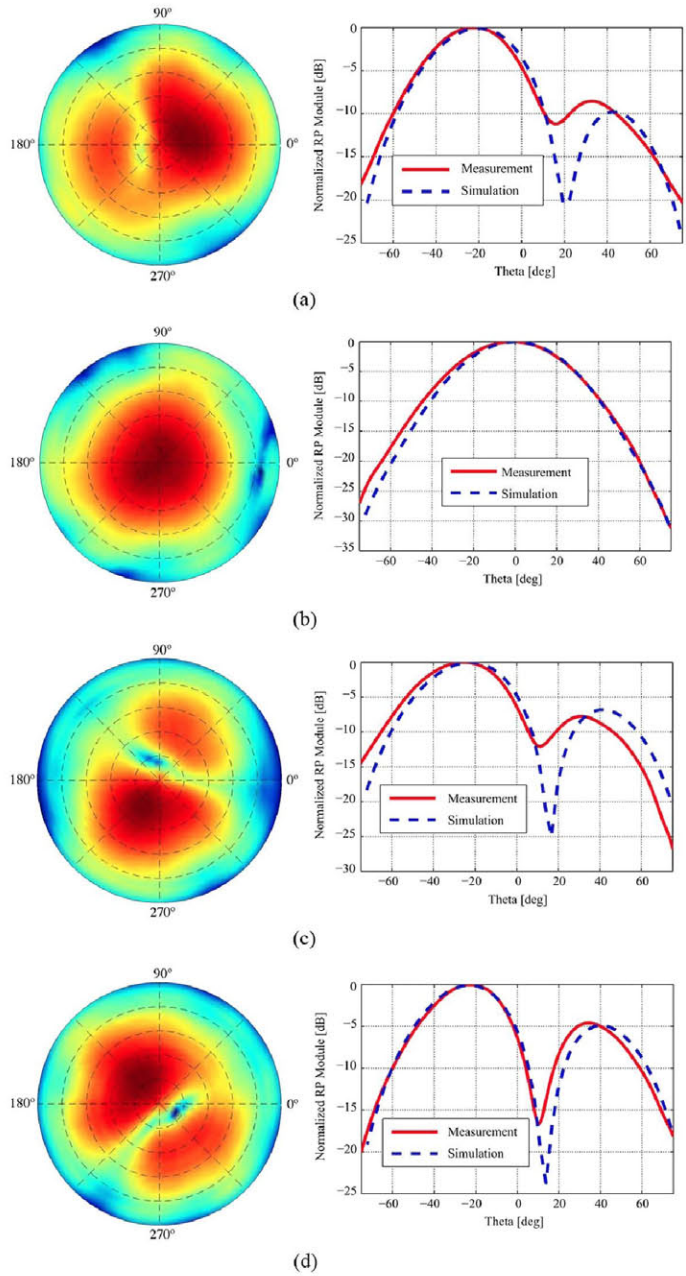

Fig. 10. (a), (b), (c), and (d) Measured radiation patterns of the beam forming network and cell subarray GEODA by exciting AI1, AI2, AI3, and AI4 respectively. (Left column) Comparison between measured (red) and simulated (blue) radiation patterns.

Considering the case under study, and taking into account the expressions above, it is shown the desired 180° rotation beams

$$\beta = 116.6° \quad \text{with } \theta_{0B} = 41.9° = -\theta_{0A}. \tag{37}$$

Losses associated with the BFN B are the same as in the simple BFN A.

The BFN B has being simulated and implemented as BFN A, obtaining a similar behavior as its complementary. After validations, the whole 7 × 3 network has being built as shown in Fig. 12. Scattering parameters of the network have being measured. Scattering parameters of the 7 × 3 network related to A-input ports are similar to those shown in Table I but 3 dB

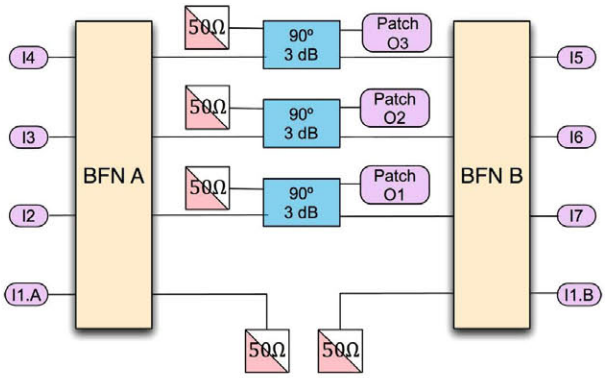

Fig. 11. 7 × 3 BFN Scheme.

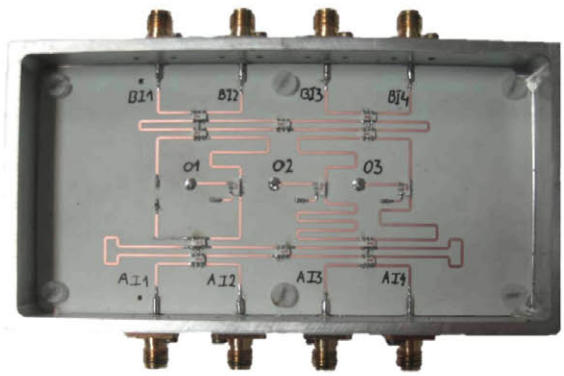

Fig. 12. Implementation of the 7 × 3 BFN.

TABLE II
SCATTERING MATRIX AND LOSSES OF THE 7 × 3 NETWORK

	Patch 1-O2	Patch 2-O3	Patch 3-O4	β	Losses
1A	$0.48e^{j0.70\pi}$	$0.21e^{-j0.65\pi}$	$0.20e^{-j0.66\pi}$	116°±1°	68%
2A	$0.21e^{-j0.19\pi}$	$0.22e^{-j0.16\pi}$	$0.20e^{-j0.17\pi}$	0°±4°	86%
3A	$0.22e^{j0.822\pi}$	$0.22e^{j0.81\pi}$	$0.46e^{j0.20\pi}$	112.1°±1°	69%
4A	$0.21e^{j0.34\pi}$	$0.48e^{-j0.28\pi}$	$0.21e^{j0.37\pi}$	113.8°±2°	68%
1B	$0.52e^{j0.95\pi}$	$0.21e^{j0.33\pi}$	$0.22e^{j0.31\pi}$	-114.3°±2°	64%
2B	$0.20e^{j0.85\pi}$	$0.23e^{j0.85\pi}$	$0.24e^{j0.83\pi}$	0°±2°	85%
3B	$0.24e^{j0.85\pi}$	$0.19e^{j0.83\pi}$	$0.53e^{-j0.53\pi}$	-113.5°±2°	63%
4B	$0.20e^{j0.34\pi}$	$0.49e^{j0.96\pi}$	$0.22e^{j0.28\pi}$	-116.5°±5°	67%

lower due to coupler combiner/divider between complementary networks. Table II summarizes measurements of scattering parameters of the whole network, where is shown ±0.3 dB error module and a ±5° error phase. Fig. 13(a) shows the measurement of the radiation pattern of the broadside beam, and Fig. 13(b) depicts the measurement of the general radiation pattern of a tilted beam. Besides, main plane sections of measured and simulated radiation patterns are also presented, showing similar characteristics as previous network A (Fig. 10). Hence, these measurements show a successful system behavior, providing desired beams.

VI. CONCLUSIONS

BFN for triangular subarrays of three radiating elements has been studied. Intrinsic features of lossless networks limit the

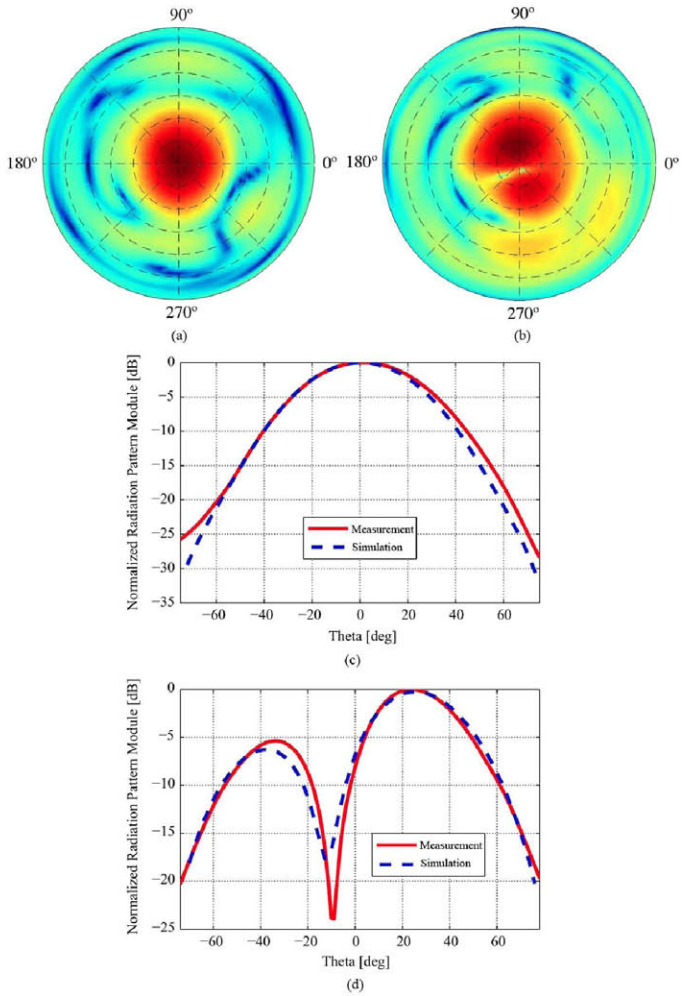

Fig. 13. Measurements of the radiation pattern of the broadside beam (a), and the general radiation pattern of a tilted beam, (b). Measured (red) and simulated (blue) sections of the main plane radiation patterns for broadside (c), and tilted (d) beams.

number of beams generated leading the investigation to dissipative network. A novel quasi-orthogonal network providing three orthogonal beams in a desired θ_0 elevation angle and an extra broadside one has being proposed. Besides, a 7 × 3 network based on two complementary of those novel beam-formers has been described. Practical implementations of both networks have been applied to GEODA triangular subarray cell. Measurements ensure a correct behavior of both systems, proving the effectiveness of the proposed innovative BFN design.

REFERENCES

[1] A. Torre, J. Gonzalo, M. Pulido, and R. M. Rodríguez-Osorio, "New generation ground segment architecture for LEO satellites," in *Proc. 57th Int. Astronautical Congr.*, Valencia, Spain, Oct. 2006, pp. 221–226.

[2] C. A. Balanis, *Modern Antenna Handbook*. New York, NY, USA: Wiley, 2008.

[3] L. C. Godara, *Smart Antennas*, 1st ed. Boca Raton, FL, USA: CRC.

[4] M. A. Salas Natera, A. García Aguilar, J. Mora Cueva, J. M. Fernández, P. Padilla Da La Torre, J. García-Gasco Trujillo, R. M. Rodriguez-Osorio, M. Sierra-Peréz, L. De Haro Ariet, and M. S. Castañer, "New Antenna Array Architectures for Satellite Communications, Advances in Satellite Communications ," in *Advances in Satellite Communications*, M. Karimi and Y. Labrador, Eds. Madrid, Spain: Universidad Politechnica de Madrid.

[5] R. Mailloux, *Phased Array Antenna Handbook*. Norwood, MA, USA: Artech House.
[6] R. O. Schmidt, "Multiple emitter location and signal parameter estimation," in *Proc. RADC Spectrum Estimation Workshop*, Griffiss Air Force Base, NY, USA, 1979, pp. 243–258.
[7] R. C. Johnson and H. Jasik, *Antenna Engineering Handbook*. New York, NY, USA: McGraw-Hill, 1984.
[8] J. García-Gasco Trujillo, M. Salas Natera, I. Montesinos, M. Arias Campo, M. Sierra Pérez, and R. Martínez, "GEODA-GRUA: Adaptive multibeam conformal antenna for satellites communications," presented at the 30th URSI General Assembly and Sci. Symp. Int. Union of Radio Sci., Istanbul, Turkey, Aug. 2011.
[9] J. García-Gasco Trujillo, M. Sierra Pérez, A. Novo García, and M. Vera-Isasa, "Multibeam network design and measurement for triangular array of three radiating elements," presented at the 5th Eur. Conf. Antennas and Propagation, Rome, Italy, Apr. 2011.
[10] B. Tomasic, J. Turtle, and S. Liu, "A geodesic sphere phased array antenna for satellite control and communication," presented at the XXVII General Assembly of the Int. Union of Radio Sci., Maastricht, The Netherlands, Aug. 2002.
[11] S. Liu, B. Tomasic, S. Hwang, and J. Turtle, "The geodesic dome phased array antenna (GDPAA) for satellite operations support," in *Proc. IEEE 18th Int. Conf. Appl. Electromagnetics and Commun.*, Dubrovnik, Croatia, Apr. 2006, p. 1.
[12] I. Montesinos, M. Sierra Pérez, J. L. Fernández, R. Matínez, and J. L. Masa, "GEODA: Adaptive antenna of multiple planar arrays for satellite communications," presented at the Eur. Conf. Antenna and Propagation, Berlin, Germany, 2009.
[13] A. K. Bhattacharyya, *Phased Array Antennas*. New York, NY, USA: Wiley.
[14] R. H. Roy and T. Kailath, "Esprit-estimation of signal parameters via rotational invariance techniques," *IEEE Trans. Acoust., Speech, Signal Process.*, vol. 37, no. 7, pp. 984–995, Jul. 1989.
[15] R. Hansen, *Phased Array Antennas*. Hoboken, NJ, USA: Wiley, 1998.
[16] J. Butler and R. Lowe, "Beam-forming matrix simplifies design of electronically scanned antennas," *Electron. Design*, vol. 9, pp. 170–173, Apr. 1961.
[17] J. Blass, "Multidirectional antenna – A new approach to stacked beams," in *IRE Int. Convention Record*, 1960, pp. 48–50, Part 1.
[18] W. Rotman and R. Turner, "Wide-angle microwave lens for line source applications," *IEEE Trans. Antennas Propag.*, vol. AP-11, no. 6, pp. 623–632, Jun. 1963.
[19] J. H. Kim, K. D. Jang, W. J. Byun, B. S. Kim, K. S. Kim, M. S. Song, and W. S. Park, "Design of a novel switched four beam array antenna for millimeter wave," in *Proc. IEEE Antennas and Propagation Soc. Int. Symp.*, Jun. 9–15, 2007, pp. 2654–2657.

Javier García-Gasco Trujillo was born in 1986 in Toledo, Spain. He received the M.Sc. degree in telecommunication engineering from the Technical University of Madrid (UPM), Madrid, Spain, in 2009.

Since then, he is a Ph.D. degree student in the Radiation Group, Signal, Systems and Radiocommunications Department, UPM. His main research interest is reconfigurable planar phased array antennas, focusing on multi-beamforming networks and transmission/reception modules for L and S bands.

Álvaro Noval Sánchez de Toca was born in Madrid, Spain, in 1986. He received the M.Sc. degree in telecommunication engineering from the Technical University of Madrid (UPM), Madrid, Spain, in 2011.

He is currently working toward the Ph.D. degree in the Radiation Group, UPM, as a recipient of a Spanish Ministry of Science and Innovation Scholarship (2011–2015). His research interests include active array antenna design with electronic steering for satellite communications. He is participating in national and international investigation.

Ignacio Montesinos-Ortego was born in León, Spain, on April 19, 1984. He received the B.S., M.S., and Ph.D. degrees in electrical engineering from Technical University of Madrid (UPM), Madrid, Spain, in 2007, 2009, and 2012, respectively.

From 2007 to 2009, was a Research Associate in the Radiation Group of UPM. From 2009 to 2011, he became a Research Associate at Ando & Hirokawa Laboratory at Tokyo Institute of Technology, Tokyo, Japan. His researching interests are planar waveguide arrays, smart antenna arrays and beam-forming networks.

José-Manuel Fernández was born in Lausanne, Switzerland, in 1977. He received the Diplôme d'Ingénieur en Électricité from the École Polytechnique Fédérale de Lausanne (EPFL), Lausanne, Switzerland, in 2003. He received the M.S. and Ph.D. degrees in electrical engineering from Technical University of Madrid (UPM), Madrid, Spain, in 2003 and 2009, respectively.

Since 2009, he is a Postdoctoral Researcher in the Radiation Group at Technical University of Madrid. His current research interest is in the field of metamaterial structures with emphasis on planar antenna applications.

Manuel Sierra-Peréz was born in Zaragoza, Spain, in 1952. He received the Master degree (Telecommunication Engineer) from the Technical University of Madrid (UPM), Madrid, Spain, in 1975 and the Ph.D. degree in 1980.

He became a Full Professor at UPM in 1990. He has lead a large number of research projects with public organizations and companies. He is the author of several books and book chapters and is a reviewer of papers on research projects. His research experience and main interest is in the area of antennas and radiofrequency circuits associated with antennas. In recent years, his main research projects dealt with the design of antenna arrays, either active or passive, and associated circuits.